Estimating surface melt and runoff on the Antarctic Peninsula using ERA-Interim reanalysis data.

Costi, Juliana; Arigony-Neto, Jorge; Braun, Matthias; Mavlyudov, Bulat; Barrand, Nicholas E.; Da Silva, Aline Barbosa; Marques, Wiliam Correa; Simoes, Jefferson Cardia

DOI:
10.1017/S0954102018000391

Estimating surface melt and runoff on the Antarctic Peninsula using ERA-Interim reanalysis data

Journal:	*Antarctic Science*
Manuscript ID	AntSci-2017-SP-1218.R1
Manuscript Type:	Standard Paper
Date Submitted by the Author:	09-Apr-2018
Complete List of Authors:	Costi, Juliana; Federal University of Rio Grande do Sul, Geosciences; Universidade Federal do Rio Grande, Instituto de Matemática, Estatística e Física Arigony-Neto, Jorge; Universidade Federal do Rio Grande Braun, Matthias; University of Erlangen-Nuremberg, Geography Mavlyudov, Bulat; Russian Academy of Sciences, Geography Barrand, Nicholas; University of Birmingham, School of Geography, Earth and Environmental Sciences Silva, Aline; Universidade Federal do Rio Grande Simões , Jefferson; Universidade Federal do Rio Grande do Sul, Centro Polar e Climático
Keywords:	Positive degree-days, meltwater, glacier and snow surface melting, ablation, runoff

Estimating surface melt and runoff on the Antarctic Peninsula using ERA-Interim reanalysis data

Juliana Costi[1*], Jorge Arigony-Neto[2], Matthias Braun[3], Bulat Mavlyudov[4], Nicholas E. Barrand[5], Aline Barbosa da Silva[2], Jefferson Cardia Simões[1].

1 Polar and Climatic Center, Institute of Geosciences, Federal University of Rio Grande do Sul, Porto Alegre, Brazil

2 Laboratory for Monitoring of the Cryosphere, Institute of Oceanography, Federal University of Rio Grande, Rio Grande, Brazil

3 Institut für Geographie, Friedrich-Alexander-University Erlangen-Nürnberg, Wetterkreuz 15, D-91058 Erlangen, Germany

4 Russian Academy of Sciences, Institute of Geography, Vavilova, 37, Moscow, Russia

5 School of Geography, Earth and Environmental Sciences, University of Birmingham, Birmingham, UK

* Currently at Laboratory of Numerical Analysis and Dynamic Systems, Institute of Statistics, Mathematics and Physics, Federal University of Rio Grande, Rio Grande, Brazil

Corresponding author: J. Costi, ju.costi@gmail.com

Abstract

Using the Positive Degree Days approach and ERA-Interim reanalysis downscaled data, we ran a melt model spatially gridded at 200 m with annual temporal resolution over 32 years and estimated surface melt and runoff on the Antarctic Peninsula. Our model was calibrated and validated independently by field measurements. The maximum surface melt values occurred in 1985 (129 Gt), and the maximum runoff (40 Gt) occurred in 1993; both parameters showed minimum values in 2014 (26 Gt and 0.37 Gt, respectively). No significant trends are present. Two widespread positive anomalies occurred in 1993 and 2006. Our results reveal that the floating ice areas produce an average of 68% of runoff and 61% of surface melt, emphasizing their importance to coastal hydrography. During the seven years preceding the Larsen B collapse, surface melt retention was higher than 95% on floating ice areas, and negative runoff anomalies persisted. Excluding the islands, the vicinity of this former ice shelf exhibits the highest specific surface melt and runoff along the studied area.

Keywords

Positive degree-days, glacier and snow surface melting, meltwater.

1 Introduction

The Antarctic Peninsula is a region that is warming far faster than the global average. Up to the millenium the annual mean air temperature has increased by 2.5-3.0°C (Turner *et al.* 2005, Trenberth *et al.* 2007, Steig *et al.* 2009). The number of days with positive air temperature and consequently the duration of melt events every year have increased **at a rate** of 0.5 ±0.3 days year^{-1} over the 1980 – 2002 period (Torinesi *et al.* 2003). This climatic scenario **increases surface melt**, which accelerated over the twentieth century (Abram *et al.* 2013). Since the millenium a significant cooling trend was observed (Turner et al. 2016) that also shows glaciological implications **(Oliva *et al* 2017).**

Surface melt (SM) has been regarded as one of the major factors associated with the breakup and disintegration of the Larsen A and B ice shelves (Scambos *et al.* 2003). Surface runoff (SR) from land-based ice masses directly and indirectly influences short-term sea-level changes. It adds freshwater to the oceans and lubricates the glacier bed, causing potential changes in and acceleration of the glacier mass flux (Pfeffer *et al.* 1991, Zwally *et al.* 2002, Vaughan 2006, Osmanoglu *et al.* 2014). Recent studies have shown that ocean temperature is the leading factor that determines large ice shelves' thinning (Pritchard *et al.* 2012). The resulting decreased buttress (Fürst et al. 2016), in turn, accelerates the ice flux of marine-terminating glaciers, resulting in a dynamic thinning much larger than the losses caused by surface melt (Wouters *et al.* 2015). Though not the main contributors to mass loss and ice shelf breakup, SM and SR are highly associated with the observed changes on the AP.

SM, SR and ice discharge from glaciers by calving are the main drivers for freshwater input in the surrounding oceans of the AP. Freshwater supplies are important components in coastal ecosystems because they influence the physical and chemical settings of the water column, affecting both the structure and the function of coastal food webs (Moline *et al.* 2004). Studies in shallow, circulation-restricted bays of King George Island showed that suspended particulate matter

transported by glacier runoff can reduce light availability in shallow waters (Schloss *et al.* 2012) and govern the availability of macro nutrients for phytoplankton production (Nędzarek 2008, Kienteca Lange *et al.* 2014). Even far from the coast, Dierssen *et al.* (2002) found phytoplanktonic blooms to be associated with glacier melt. **Hodson et al. (2017) reported the occurrence of biologic activity hotspots associated to iron enrichment supplied by glacial weathering**.

Previous studies investigated SM and SR on AP primarily through remote sensing and regional climate modelling. Using passive microwave data (1978-present), studies addressing changes in melt extent, duration and water amounts could not find a significant temporal trend. However, these studies note decreasing, though statistically insignificant, trends for melt extent, melt index and total annual melt (Torinesi *et al.* 2003, Liu *et al.* 2006a, Kuipers Munneke *et al.* 2012, Trusel *et al.* 2013). The only positive trend in melt duration was found by Torinesi *et al.* (2003) from 1980 to 2000. They found that melting lasts for an average of 50 days on the AP, reaching a maximum of 100, with an increasing trend of 0.5±0.3 day $year^{-1}$ (1980-1999). Liu *et al.* (2006) determined a median melt duration of 59 days with an absolute variation of 5.39 days and a melt extent ranging from 2.5x105 km^2 to 3.5x105 km^2. Barrand *et al.* (2013) combined remote sensing observations and simulations from the regional model RACMO2 to investigate melt conditions, finding melt extents ranging from $2.8x10^5$ km^2 to $3.3x10^5$ km^2 (QuickSCAT) and $1.8x10^5$ km^2 to $3x10^5$ km^2 (RACMO2 regional atmospheric model) from 2000 to 2009.

Quantitative estimates of melt rates or freshwater input to the ocean are even scarcer. Van de Berg *et al.* (2005) showed a maximum annual melt of 0.5 m water equivalent (w.e.) yr^{-1} occurring on the Larsen ice shelf's northern edge from 1958 to 2002. Vaughan (2006) estimated values for SM in the year 2000 tof 54±26 Gt (450±216 mm we). He considered only the grounded ice portion of the AP and predicted an increase in SM to 100±46 Gt for 2050 assuming the current increasing trend of annual mean air temperature. Hock *et al.* (2009) estimated that from 1961 to 2004, an increase in the sea level of 0.22±0.16 mm yr^{-1} resulted from the contribution of mass loss

from glaciers and ice caps surrounding Antarctica, mostly AP. More recently, Kuipers Munneke *et al.* (2012) found SM values ranging from 20 to 130 Gt yr^{-1} for the AP. The analysis considered the entire Antarctic ice sheet and surrounding ice shelves, from 1979 to 2009, and showed no statically significant decreasing trend.

In this study, we present comprehensive estimates for surface melt and runoff on the Antarctic Peninsula and surrounding islands. We run a Positive Degree Day-based glacier melt model adapted from Vaughan (2006) and Pfeffer *et al.* (1991), driven by data from the global reanalysis project ERA-Interim (ERAI) from the European Center for Medium-range Weather Forecast (ECMWF). We calibrate and validate the model via a multi-criteria scheme using in-situ observations and long-term surface mass balance records. Our model runs cover the 1981-2014 period.

2 Study site

The AP is a region with strong latitudinal and longitudinal gradients of climatic parameters (Morris & Vaughan, 2003). The central mountain range, reaching more than 2000 m a.s.l., forms a major obstacle in the southern hemisphere polar vortex (Fig. 1). Although the climate of the AP west coast and adjacent islands is cold maritime, the conditions are much more continental on the east coast and further south. Consequently, summer melt regularly occurs along the west coast at lower elevations. Frequent warm foehn-type winds on the east coast are known to cause considerable surface melt, and cold barrier winds lead to cold air mass outbreaks from the Filchner-Ronne Ice Shelf along the AP's mountains to the north. Such foehn events impact the surface temperature regionally in time scales varying from hours to seasons (Cape et al., 2015). Larsen-C/D, Wilkins and George-VI ice shelves are the largest low-elevation areas. The plateau of the Antarctic Peninsula is dominated by a dry snow zone, indicating mean annual surface temperatures

below -11°C (Rau & Braun 2002). Large mountain glaciers drain from the plateau to both sides of the AP. The small islands surrounding the peninsula are covered by ice caps and ice fields.

3 Data

The AP does not have a well-distributed weather station network with long time series (see Fig. 1). In this case, a feasible alternative to the spatial interpolation of uneven observations is to use data provided by reanalysis projects. Such datasets incorporate available observations to minimize the errors of the prediction model.

ERAI is a reanalysis product from ECMWF. It provides data from 1979 to the present in a finest spatial resolution of approximately 0.7º. Compared with previous versions, such as ERA-40 and ERA-15, the temperature bias over Antarctica **has been** reduced. The orography in the model is an average of finer resolution digital elevation models, such as GTOPO30 (Gesch *et al.* 1999). This averaging smoothes the highly complex topography of the AP.

To better represent the topography, we used the RAMP DEM (Liu *et al*. 2001) as the input for an altitudinal lapse-rate downscaling method, which was evaluated using near surface air temperature data from 28 weather stations. The resulting grid cell size after downscaling was 200 m x 200 m.

Direct ablation measurements were available from 3 sources: (i) Measurements in 10-14 day intervals at 29 mass balance stakes during the austral summer from 2007 to 2012 at the Bellingshausen Dome in King George Island – South Shetland Islands (Stake line 1) (Tab. 1; Mavlyulov 2014). (ii) Continuous surface melt measurements available from a sonic ranging sensor (SR50) operated over 42 days of the 1997/98 austral summer at daily intervals (Braun *et al*, 2001; 2004). . (iii) Mass balance stakes readings during summer field campaigns (Stake line 2). These

measurements were conducted during two summer seasons (1997/1998 and 1999/2000) on the Bellingshausen Dome (Braun *et al*, 2001; 2004).

Spatially-integrated summer and winter mass balances of the Hurd and Johnsons glaciers in Hurd Peninsula, Livingston Island were available for 10 years (Navarro *et al.* 2013, data provided by the World Glacier Monitoring System). A 14-year record of the annual surface mass balance of Glaciar Bahia del Diablo, Vega Island was used as a quantitative reference for the northeastern AP region (Skvarca *et al.* 2004, Marinsek & Ermolin 2015).

4 Methods

4.1 ERA-Interim temperature downscaling

To account for the spatiotemporal variation in the air temperature altitudinal lapse rates along the study area, we computed the temperature and geopotential height differences between the 1000 hPa and 750 hPa pressure levels. Thereafter, we calculated the ratio between the two differences for each day and grid element and applied the given lapse rate (eq. 1) to the elevation difference between the RAMP-DEM and the ERAI geopotential height at the surface (eq. 2). The result was then reduced from the temperature at 2 m (eq. 3).

$$lr(\phi, \lambda, d) = \frac{T_{1000}(\phi, \lambda, d) - T_{750}(\phi, \lambda, d)}{h_{1000}(\phi, \lambda, d) - h_{750}(\phi, \lambda, d)} \quad \text{(eq. 1)}$$

$$dh = h_{ERA-sfc} - h_{RAMP-DEM} \quad \text{(eq. 2)}$$

$$T_{DS}(\phi, \lambda, d) = T_{2m}(\phi, \lambda, d) + (dh(\phi, \lambda, d) \square lr(\phi, \lambda, d)) \quad \text{(eq. 3)}$$

where *lr* is the lapse rate, T_{1000}, T_{750}, h_{1000} and h_{750} are the temperatures and geopotential heights at 1000 hPa and 750 hPa, respectively, $h_{ERA\text{-}sfc}$ is the geopotential height of the surface, $h_{RAMP\text{-}DEM}$ is the elevation given by RAMP DEM (Liu *et al*. 2001), T_{DS} is the temperature downscaled, T_{2m} is the temperature 2 m above the surface, φ and λ are the latitude and longitude, and d is the day. For each model grid cell, we used the ERAI cell with the cell centre closest to the model grid centre.

It is worth noting that the lapse-rate method for air temperature downscaling only accounts for the decrease of the air temperature due to the vertical variation inside the ERA-Interim grid elements. It does not include any further dynamic process that may affect the air temperature which are not already represented in the ERA-interim global climatic model. It also represents the free atmosphere and does not account for any local effects or boundary-layer processes.

4.2 Surface melt (SM) and runoff (SR) computations

The positive degree day (PDD) is the sum of daily positive near surface air temperatures during a given period (in this case, one year) **(Vaughan, 2006)**. When multiplied by a melt factor (MF), it provides the total SM:

$$SM(\phi,\lambda,d) = MF \sum_{d=1}^{d=365} T_{DS}(\phi,\lambda,d)\alpha(\phi,\lambda,d) \qquad \text{(eq. 4)}$$

$$\begin{cases} \alpha(\phi,\lambda,d) = 1, if T_{DS}(\phi,\lambda,d) > 0 \\ \alpha(\phi,\lambda,d) = 0, if T_{DS}(\phi,\lambda,d) < 0 \end{cases}$$

where d is the first day of the annual melting periods (October 1st in this case), d is the number of days in the same period, and T_{DS} is the daily mean of the near surface air temperature. .

The energy balance at the surface implies that melt can occur when the air temperature is equal or below 0°C, and even not occur when the temperature is positive. In this sense, the 0°C

threshold for melt occurrence may be considered an artificial threshold. In order to determine the more suitable threshold, we ran our model considering 5 different thresholds for the same period covered by the study of Barrand et. al (2013), i.e., from 1999 to 2002. We then compared the mean melt duration of the period as estimated by our model against the QuickSCAT-derived estimates obtained by Barrand et al (2013). Besides the classical PDD approach, which considers that melt occurs when the air temperature is positive, we also considered that melt can occur when the air temperature is equal to and above 0°C, above -1°C, above -0.5°C, above 0.5°C and above 1°C. The latter two thresholds were tested in order to account for the known overestimation of the ERAI-derived air temperature on the AP.

SR is calculated as the difference between SM and the amount of meltwater retained in the snowpack through refreezing, pore filling and capillarity:

$$SR = SM - M_0 \qquad \text{(eq. 5)}$$

with M_0 given by (Pfeffer *et al.* 1991)

$$M_o = \frac{c}{L} C T_f + (C - SM)\left(\frac{\rho_{pc} - \rho_c}{\rho_c}\right) \qquad \text{(eq. 6)}$$

where c is the heat capacity of ice, L is the latent heat of fusion of ice, C is the snow accumulation, T_f is the temperature of the firn at the beginning of the melt season (in positive Celsius degrees below the freezing point), is the initial firn density (taken as 400 kg m^{-3}) and ρ_{pc} is the pore close-off density (taken as 830 kg m^{-3}). After **setting** ρ_c = 400 kg m^{-3} and ρ_{pc} = 830 kg m^{-3} (Vaughan 2006), M_0 we get

$$M_o = \left(0.003 T_f + 0.52\right) C \qquad \text{(eq. 7)}$$

After assuming that T_f is the mean air temperature of the previous year in each grid cell, the only unknown variable for calculating M_0 is C. We approximate C as the annual accumulation for each grid element given by ERAI (resampled by nearest neighbour to the model grid). Hence, we

estimate the accumulation and temperature-driven changes in retention for each year, and we estimate the SR **using eq. 5.**

4.3 Calibration and validation of the model

We applied a multi-criteria calibration and validation scheme with rigorous data splitting for model calibration, **data** downscaling and model validation.

To validate the downscaling approach, we compared monthly PDDs computed from the downscaled ERAI data and from weather station data (records longer than 10 years). The analysis was restricted to the months from October to March **to focus on the melt periods**. The PDDs correlation strength and the sum of errors were utilized as quality indicators.

The melt model was calibrated by tuning the **melt factor** using ERAI downscaled data in equation 4 to achieve an optimal **fit to** the ablation records (N=300) of stake line 1. A melt factor of 5.4 mm w.e. K d^{-1} was determined with r^2=0.65 using all available records. When stakes are considered individually, the **melt factor takes** values between 2.2 mm and 12.6 mm w.e. K d^{-1} (although both **of them** are extreme values). The **melt factor** is well within the range reported for comparable arctic regions and at the upper bound for Antarctica (Huybrechts & Oerlemans 1990, Braithwaite & Zhang 2000, Hock 2003).

Independent validation of the model performance was carried out using a variety of datasets at different locations and different time intervals. We compared the melt rates at stake line 2 and the SR50 continuous record over a 6-week melt period, both on King George Island. The surface mass balance records provided an integrated error estimate for summer and winter (Livingston Island) (Navarro *et al.* 2013) or an entire glacier mass balance year (Vega Island) (Skvarca *et al.* 2004, Marinsek & Ermolin 2015).

5 Results

5.1 PDD threshold and spatial representation of the mean melt duration (MMD).

By spatially comparing the annual mean melt duration from 1999 to 2002 (Fig. 2), we observe that the best performance is achieved **when using** the 0°C threshold. **The energy balance at the surface determines that melting can occur at temperatures below 0°C. However, the comparisons made between the ERAI-derived and the weather stations-derived PDDs (section 5.2, Tab.3) show that both are very well correlated, although the absolute values are overestimated. This may explain the best performance of the 0°C threshold for determining the MMD, although it could be expected that a lower temperature would result in a better representation of the MMD.**

5.2 Downscaling and melt model performance

The ERAID-derived PDDs showed very good agreement with weather station data. Correlation coefficients ranged from 0.58 to 1.0, with the majority above 0.9 (Tab. 3). Nevertheless, absolute values were overestimated by ERAID**-derived data**.

We validated the SM using two other independent point ablation measurements carried out in the Bellingshausen Dome (Stake line 2 and SR50). Compared to these datasets, the modelled SM produced a slight underestimation of the surface ablation. After 41 days of ablation monitoring with the SR50, we found a final difference of 80 mm w.e. between the modelled and the measured ablation. **The RMSE was 7.19 mm w.e., and the bias was 4.9 mm w.e. The linear correlation of**

our ablation estimates with Stake line 2 was 0.86 (Fig. 3), with RMSE of 19.08 mm w.e. and bias of 7.14 mm w.e..

We compared our SM estimations in the Hurd Peninsula (Livingston Island) to measurements carried out by Navarro *et al.* (2013) on the Hurd Glacier (HG) and Johnsons Glacier (JG) from 2002 to 2011 (Fig. 4). The same study also measured the winter accumulation, which we used to evaluate the accumulation estimate over the same periods. The correlation of the modelled ablation with HG was 0.61 and with JG was 0.68**, with RMSE of 158 mm w.e.**. The accumulation correlations were 0.8 (HG) and 0.49 (JG), **with RMSE of 247 mm w.e**. . Values always ranged on the same scale and did not show a fixed over- or underestimation,. Additionally, we estimated the annual surface mass balance of Glaciar Bahia del Diablo (Vega Island) and compared it to field measured data from this site (Skvarca *et al.* 2004, Marinsek & Ermolin 2015). The error was **lower** than 200 mm w.e. **for** 9 of the 13 analysed years, the correlation between the measured and the modelled SMB was 0.67, and the **RMSE was 214 mm w.e..**

The average ablation was underestimated in the SR50 and SL2 validation site, respectively 0.14 mm we (2% below the observation) and 11.4 mm we (20% above the observation). The average summer ablation of Livinston Island was overestimated in 120.45 mm we (17% above the observation), whereas the winter accumulation was overestimated in 107.69 mm we (16% above the observation). The annual mass balance of the Bahía del Diablo glacier was overestimated in 30.52 mm we (20% above the observation). The best correlation between the modeled and the observed time series was found with the SL2 observations, which is expected as the SL2 is located at the MF calibration site. Although the SR50 measurements were also performed at the calibration site, the PDD method is acknowledged for its poorer performing on the daily time scale when compared to longer time scales.

The observational data available for validating this study is composed by measurements performed in time intervals ranging from daily to annual, implying in different magnitudes of abblation, accumulation and mass balance. To account for the diverse measurement magnitudes, we computed the normalized RMSE considering the range of the observed measurements. The normalized RMSE ranged from 0.16 to 0.25, with the lowest value associated to the SL2 validation site and the highest value associated to the winter accumulation on Livingston Island. It was expected that the model would have a worst performance out of the melt factor calibration site because melt factors tipically vary in regions as large as the Antarctic Peninsula. However, a better comparison of errors would require longer measurements carried out in similar time scales.

5.3 Surface melt and runoff time series

The annual time series for the mean near surface air temperature and PDDs and the total SM, Mo and SR are presented in Figure 5 for the total, grounded and floating areas of the AP. The years correspond to the melt season that started in November of the previous year.

The mean near surface air temperature does not represent the PDDs' interannual variability. Both series show $r^2 = 0.11$, which is not surprising considering there are no PDDs during most months that compose the annual mean temperature.

Total SM had maximum values in 1985 (129 Gt) and 1993 (127 Gt) and a minimum value in 2014 (26 Gt). The mean and standard deviation values for the entire period and area were 75±54 Gt, or 46±15 Gt and 25±8 Gt when considering **separately** floating and grounded areas, respectively. SR had a maximum value in 1993 (40 Gt) and a minimum value in 2014 (0.37 Gt), with a mean 9±8 Gt and, for floating and grounded areas, 5±6 Gt and 3±2 Gt, respectively.

Since 2008, both SM and SR have persistently shown negative anomalies considering the

entire period. The same happened from 1996 to 2002 but only for SR. The period 1996 to 2002 is also characterized by a lower interannual variability in the mean air temperature, PDDs and SM, whereas M_0 has not shown the same behaviour. Hence, the decoupling of SR and SM for this period might be associated with high accumulation rates.

The spatial distribution of the mean and standard deviation of SM and SR is presented in Figure 6. The effects of foehn winds are clearly reflected in the mean SM (Fig. 6-a) for the western border of the Larsen C ice shelf (LCIS), showing that these types of events are large and persistent enough to be represented in a global reanalysis.

5.4 Surface melt and surface runoff regions

We divided the AP in 11 sub-**regions** to analyse the spatial SM and SR variations in the major drainage basins and ice shelves, bays and topographical features. **Because** the areas of the regions considered are **different**, we computed the specific SM and SR (SM/A and SR/A, in **m w.e.**; Fig. 7). The largest SM/A and SR/A correspond to the South Shetland Islands (SSI). Excluding the islands, SM/A and SR/A are larger in the E-LB region.

The regional SM/A time series have a higher correlation than **the** SR/A time series. Most areas' SM/A and SR/A are better correlated with the immediate neighbour area **to the east or the west sides.** The northern areas (W-N1, W-N2, E-N and E-LB) and northern islands (SSI and Joi) show very similar SM and SR temporal behaviours; the differences strongly reflect the elevation profiles. E-N shows a higher correlation with SSI (0.91) and Joi (0.91) than W-N1 (0.86 and 0.74, respectively). E-LC correlates better with E-LB, although the absolute amounts are considerably smaller. E-S correlates better with W-S than any other region, showing that there is a more pronounced climatic difference, in terms of interannual variability, between the regions in the E-LC latitude range.

The distribution of the SM and SR along the elevation profiles reveals that more than 90% of the SM/A (SR/A) is produced at elevations between 0 m and 500 m (400 m). This proportion decreases with elevation in all regions, except for the E-LC. In this area, SM/A is higher in the elevation range of 100 to 200 m than 0-100 m. The occurrence of foehn-type winds in this area leads to higher temperatures near the border with the grounding line, increasing melt.

SR/A is better distributed along the profile, and 90% occurs below an altitude of 400 m. The SSI and the Joi also show similar distribution patterns. The W-Wi and the W-S have 45% and 50% of SM/A, respectively, restricted to 0-100 m. The W-MB shows 90% of SR/A restricted to 0-200 m. **The greatest difference is found** between the northern regions (E-N, E-LB, W-N1, W-N2, SSI and Joi) and the southwestern regions (W-S, W-MB and W-Wi). E-S has a distribution with characteristics between both. E-LC is a special case, where more melt is produced between 100-200 m a.s.l. than between 0-100 m a.s.l., as a result of foehn-type winds.

6 Discussion

The high correlation between ERAID-derived and **weather stations**-derived PDDs demonstrates the consistency **of the temporal variability of the modelled PDDs**. On the other hand, very high RMSEs show that the PDDs absolute values are not well represented by ERAID. An overestimation of air temperature over Antarctica is recognized in previous ERA datasets (van de Berg *et al.* 2005), which is also observed by our study.

The comparative analysis between the ERAI-derived MMD and the QuickSCAT-derived MMD (Barrand et al., 2013) showed that the first is underestimated on **high-slope** areas and overestimated on the northern tip of the Larsen-C ice shelf. The terrain slope is a major difficulty for atmospheric models and even for remote sensing data processing. **Therefore**, a worst performance in **high-slope** areas is expected. Besides that the northern Larsen C MMD

overestimation occurs in flat areas, it may also be related to a topography-related problem. The **northwestern** Larsen C is influenced by foehn-type winds, whose proper modelling is highly dependent on accurate representation of terrain elevation.

However, it is also worth noting that Luckman et al. (2014) compared Envisat/ASAR melt duration maps with the same QuickSCAT-derived data (Barrand et al., 2013), and found melt durations up to 25 days longer than the latter. The authors attribute this difference to the different spatial resolution of both datasets in the region of Larsen C influenced by foehn-type winds. **This suggests** that perhaps the QuickSCAT reference data is actually underestimating the melt duration in **Larsen C**, which would **indicate** that the MMD found in the present study is less overestimated.

Our approach for tuning the melt factor to ERAID PDDs using in-situ ablation measurements allowed for a compensation of the PDDs overestimation. Both the SM temporal variability and absolute SM values are consistent with the SR50 measurements. Our 80 mm w.e. underestimation over 40 days is acceptable, particularly considering that we used a simple approach applied to global reanalysis data. We also found a small underestimation and good correspondence with SL2 ablation measurements. The comparisons with integrated SMB from Hurd Peninsula and Glaciar **Bahía** del Diablo show that our results are reliable for a **regional-scale** analysis on the northern AP. However, it should also be noted that we have no quantitative melt or surface mass balance data to assess the quality of our products for more southern sites on the AP.

A remaining bias from the PDD overestimation not compensated for by the MF tuning would result in a larger melt area. However, the spatial distribution of PDDs is in agreement with recent works addressing the melt occurrence in AP through QuickScat and regional modelling (Kuipers Munneke *et al.* 2012, Barrand *et al.* 2013, Trusel *et al.* 2013, van Wessen *et al.,* 2016). In some regions, our data indicates a smaller melt area, which can be attributed to the enhanced resolution of our grid after the ERAI temperature downscaling. QuickScat data have spatial resolution of 5 km and RACMO2.3 of 5.5 km, whereas our temperatures were downscaled to a 200 m x 200 m grid.

Both SM and SR spatial distribution and time series are generally in good agreement with the most recent studies addressing surface melt patterns in the AP (Tedesco & Monaghan 2009, Kuipers Munneke *et al.* 2012, Barrand *et al.* 2013, Trusel *et al.* 2013, Välisuo *et al.* 2014, van Wessen *et al.*, 2016), but the absolute values are higher than those presented by previous studies. **Nevertheless, comparisons of surface melt derived from RACMO with 27 km resolution against QuickSCAT derived data showed an underestimation of SM, melt onset date and melt season duration by RACMO (Kuipers Munneke *et al.* 2012, Barrand *et al.* 2013, Trusel *et al.*2013). van Wessen *et al* (2016) presents estimates of SM provided by RACMO with 5.5 km resolution considerably smaller than those obtained by the previous model version. Comparisons of QuickSCAT-derived melt area on Larsen C against higher resolution Envisat-ASAR derived data further suggest that even QuickSCAT-derived melt area is underrepresented in the area. Such discrepancies between the different studies depicts the high uncertainties involved in modeling mass balance terms in Antarctic Peninsula**.

The effects of foehn-type winds are visible in the distributed mean SM , contrasting with their poor representation in previous modeling studies (Kuipers Munneke *et al.* 2012, van Wessen et al. 2016). In general, our SM time series agrees well with the temporal behaviour of the SM time series estimated by Kuipers Munneke *et al.* (2012) for the AP. In spite of the uncertainties associated with our approach, the results are consistent with direct field measurements (Figs. 2 and 3) and with previous.

Wouters *et al.* (2015) found a total mass loss of 300 Gt from 2000 to 2014. The study comprised the grounded portion of the AP southern sector. During the same period, and considering the grounded area of the entire AP, losses by SR were 95 Gt. The contributions of the mass losses by SR to glacier thinning and possible sea-level rise are thus small compared to ice-flux acceleration and increased calving. Nevertheless, the role of the floating areas as a direct freshwater source to the adjacent ocean is remarkable. While they comprise 24% of the total area, produce 68%

of the mean SR and 61% of the mean SM. Additionally, the fate of the liquid water is different from the fate of the ice when entering the ocean, and it impacts water's physic-chemical characteristics and biota differently.

The AP floating area has reduced in extent by 18% since 1950 (Cook & Vaughan 2010). This reduction is progressively advancing southwards. The sea-level rise around the AP, predominantly driven by stheric expansion (Rye *et al.* 2014), suggests that the oceanic forcing will continue leading to further and more dramatic ice shelf disintegration. In the future, it is likely that the melting area of the AP will be further reduced. Both LCIS and the Wilkins ice shelf are the main SM and SR sources and are partially unstable. It is predicted that the LCIS will soon undergo a large calving event caused by the development and propagation of a rift, which will remove between 9% and 12% of its area (Jansen *et al.* 2015). After a large breakup event in February 2008, the 3100 km^2 of the northern portion of the Wilkins ice shelf was at risk of collapse (Braun *et al.* 2009). A narrow ice bridge collapsed later, in April 2009 (Humbert *et al.* 2010). Consequently, ice shelf breakups may reduce the absolute amounts of water input to the ocean in the form of SR.

The accumulation rate on the AP has doubled since 1850 (Thomas *et al.* 2008), which, according to the Pfeffer *et al.* (1991) approach, increases meltwater retention. Nevertheless, Abram *et al.* (2013) showed that SM intensified much faster. The melt intensity recorded in the ice core analysed by the authors increased from 0.5% to 4.9% over the 20^{th} century. The grounded area presently retains an average of 91% of the SM, which will reduce if the observed trends continue; this may lead to an increase in the maximum height where SR occurs and an increase in SR intensity at lower elevations.

It is possible to differentiate the SM/A and SR/A time series in the 11 regions, even though the model is fed by global reanalysis data. The temperature downscaling using altitudinal lapse-rates variations in space and time allowed for a East-West differentiation in the northern tip of the AP. W-N2 region lies on the same latitude range of E-LB, and it shows SM/A and SR/A

approximately 50% lower than the latter region. The difference may be explained by topographic control (E-LB has a mean elevation 330 m lower) and smaller altitudinal temperature lapse rates on the east side of the AP (Morris and Vaughan, 2003; this study).

The analysis of SM/A and SR/A altitudinal distribution in the regions revealed that they are determined, concomitantly, by the **latitudinal** range and E-W climatic differences. Though the western side is warmer, the southwestern regions show the worst distribution due to the cold climate and higher temperature altitudinal lapse rates. Due to higher accumulation rates in the west, SR is even more restricted to **low-elevation** areas.

Two positive anomalies for both SM and SR, widespread through all regions, took place in 1993 and 2006. They coincide with the highest melt index and melt extent found by Tedesco & Monaghan (2009) for the entire Antarctic continent and are associated with the Southern Annular Mode (SAM) and Southern Oscillation Index (SOI) negative anomalies. It demonstrates the AP SM and SR are closely linked to global climatic patterns and oscillations but remain poorly known on the local spatial scales.

7 Conclusions & outlook

Using the global reanalysis ERAI, we ran a PDD-based model for SM and SR estimation, calibrated and validated with local measurements. Our results are in good agreement with previous local, regional and continental studies and can be used to reasonably investigate the combined influence of latitudinal, longitudinal and elevation differences along the **Antarctic Peninsula** on **the spatio-temporal variability of SM and SR.** Our ERAI-derived distributed PDDs are strongly correlated with **weather station**-derived PDDs. By applying **a melt factor** of 5.4 mm PDD^{-1}, we found good agreement with local measurements of SM.

The entire 1981-2014 period averages are 75 Gt (SM) and 9 Gt (SR), with a very high interannual variability (σ_{SM} = 54 Gt and σ_{SR} = 8 **Gt**). Although previous studies have found an exponential relation between PDDs and annual mean air temperature, we observe that the PDDs' interannual variability (and thereafter the value of SM) is not well represented by the mean air temperature. Maximum values occurred in 1985 for SM (129 Gt) and 1993 for SR (40 Gt). Since 2008, both variables have shown persistently negative anomalies, with minimum absolute values occurring in 2014 (SM = 26 Gt, SR = 0.37 Gt). Nevertheless, no statistically significant temporal trends are present in our time series.

From 1996 to 2002, we observe persistent negative anomalies only for SR. During this period, SM retention was always above 95% on the post-2002 floating ice areas. We suggest that this persistent high retention is possibly linked to the Larsen B breakup mechanisms that took place in 2002. The post-2002 floating ice areas are responsible for an SR average of 68% on the AP, highlighting their key importance to coastal hydrography as a freshwater source.

By dividing the AP into 11 regions, we observe that the **largest SM/A and SR/A** occur in the South Shetlands Islands, followed by the vicinity of the Larsen B ice shelf. This finding reveals the importance of the elevation and climatic differences between the western and eastern **sides of the AP**. Due to Larsen-C Ice Shelf, the east side has a flatter elevation profile, but generally also a smaller altitudinal decrease rate in temperature and lower accumulation rates than the west side, resulting in higher SM/A and SR/A in the east, despite the higher warming trends recorded in weather stations located in the west.

The large discrepancies among studies considering the same area and period indicate that further efforts are required to provide a better spatial distribution of field-measured SMB data. The same recommendation can be made for weather stations. The discrepancies are possibly due to the high complexity of global, regional and local climatic forcing combined with the equally complex internal structure of the snow and ice layers.

8 Details of data deposit

The new data presented in this paper will be archived at the PANGAEA data server (www.pangaea.de). PANGAEA is an information system hosted by the Alfred Wegener Institute, Helmholtz Center for Polar and Marine Research (AWI) and the Center for Marine Environmental Sciences, University of Bremen (MARUM).

Acknowledgements

Funding for this work was provided by EU FP7-PEOPLE-2012-IRSES IMCONet grant 318718, the Brazilian Coordination for the Improvement of Higher Education Personnel (CAPES) and the Brazilian National Institute of Science and Technology of the Cryosphere (INCT da Criosfera). M.B. was also funded via the German Research Foundation (grants BR2105/9-1 and BR2105/13-1). The RAMP DEM was kindly provided by NSIDC. Weather stations data were downloaded from NOAA at the website http://www.ncdc.noaa.gov/. ERA-Interim data were provided by the ECMWF. The surface mass balance data of Vega Island were kindly provided by S. Marinsek (Instituto Antártico Argentino). The WGMS provided surface mass balance data of Livingston Island.

Workshare

J.C. conducted all data analyses and wrote major parts of the paper. M.B. and B.M. provided in-situ reference data. N.B. provided the QuickSCAT-derived melt maps. A.S.B. calculated the differences of the mean melt duration derived from the runs of our model and from QuickSCAT data. J.C., J.A.-N. and M.B. jointly led the study. All authors contributed to and revised the manuscript.

References

ABRAM, N.J., MULVANEY, R., WOLFF, E.W., TRIEST, J., KIPFSTUHL, S., TRUSEL, L.D., VIMEUX, F., FLEET, L. & ARROWSMITH, C. 2013. Acceleration of snow melt in an Antarctic Peninsula ice core during the twentieth century. *Nature Geoscience*, **6**, 404–411, 10.1038/ngeo1787.

BARRAND, N.E., VAUGHAN, D.G., STEINER, N., TEDESCO, M., KUIPERS MUNNEKE, P., VAN DEN BROEKE, M.R. & HOSKING, J.S. 2013. Trends in Antarctic Peninsula surface melting conditions from observations and regional climate modeling. *Journal of Geophysical Research: Earth Surface*, **118**, 315–330, 10.1029/2012JF002559.

BRAITHWAITE, R.J. & ZHANG, Y. 2000. Sensitivity of mass balance of five Swiss glaciers to temperature changes assessed by tuning a degree-day model. *Journal of Glaciology*, **46**, 7–14.

BRAUN, M. & HOCK, R. 2004. Spatially distributed surface energy balance and ablation modelling on the ice cap of King George Island (Antarctica). *Global and Planetary Change*, **42**, 45–58, 10.1016/j.gloplacha.2003.11.010.

BRAUN, M., HUMBERT, A. & MOLL, A. 2008. Changes of Wilkins Ice Shelf over the past 15 years and inferences on its stability. *The Cryosphere Discussions*, **2**, 341–382, 10.5194/tcd-2-341-2008.

BRAUN, M., SAURER, H., VOGT, S., SIMOES, J.C. & GOSSMANN, H. 2001. The influence of large-scale atmospheric circulation on the surface energy balance of the King George Island ice cap. *International Journal of Climatology*, **21**, 21–36, 10.1002/joc.563/pdf.

CAPE, M.R., VERNET, M., SKVARCA, P., MARINSEK, S., SCAMBOS, T. & DOMACK, E. 2015. Foehn winds link climate-driven warming to ice shelf evolution in Antarctica. *Journal of Geophysical Research: Atmospheres,* **120**, 11.037 – 11.057, 10.1002/2015JD023465.

COOK, A.J. & VAUGHAN, D.G. 2010. Overview of areal changes of the ice shelves on the Antarctic Peninsula over the past 50 years. *The Cryosphere*, **4**, 77–98, 10.5194/tc-4-77-2010.

DIERSSEN, H.M., SMITH, R.C. & VERNET, M. 2002. Glacial meltwater dynamics in coastal waters west of the Antarctic Peninsula. *Proceedings of the National Academy of Sciences of the United States of America*, **99**, 1790–1795, 10.1073/pnas.032206999.

GESCH, D.B., VERDIN, K.L. & GREENLEE, S.K. 1999. New Land Surface Digital Elevation Model Covers the Earth. *Eos, Transactions of American Geophysical Union*, **80**, 69–70.

HOCK, R. 2003. Temperature index melt modelling in mountain areas. *Journal of Hydrology*, **282**, 104–115, 10.1016/S0022-1694(03)00257-9.

HOCK, R., DE WOUL, M., RADIC, V. & DYURGEROV, M. 2009. Mountain glaciers and ice caps around Antarctica make a large sea-level rise contribution. *Geophysical Research Letters*, **36**, 1–5, 10.1029/2008GL037020.

HODSON, A., NOWAK, A., SABACKA, M., JUNGBLUT, A., NAVARRO, F., PEARCE, D., ÁVILA-JIMÉNEZ, M.L., CONVEY, P. & VIEIRA, G. (2017). Climatically sensitive transfer of iron to maritime Antarctic ecosystems by surface runoff. Nat. Commun., 8, 14499, doi:10.1038/ncomms14499.

HUMBERT, A., GROSS, D., MÜLLER, R., BRAUN, M., VAN DE WAL, R.S.W., VAN DEN BROEKE, M.R., VAUGHAN, D.G. & VAN DE BERG, W.J. 2010. Deformation and failure of the ice bridge on the Wilkins Ice Shelf, Antarctica. *Annals of Glaciology*, **51**, 49–55, 10.3189/172756410791392709.

HUYBRECHTS, P. & OERLEMANS, J. 1990. Response of the Antarctic ice sheet to future greenhouse warming. *Climate Dynamics*, **5**, 93–102.

JANSEN, D., LUCKMAN, A. J., COOK, A., BEVAN, S., KULESSA, B., HUBBARD, B. & HOLLAND, P.R. 2015. Brief Communication: Newly developing rift in Larsen C Ice Shelf presents significant risk to stability. *The Cryosphere*, **9**, 1223–1227, 10.5194/tc-9-1223-2015.

KIENTECA LANGE, P., TENENBAUM, D.R., TAVANO, V.M., PARANHOS, R. & CAMPOS, L. DE S. 2014. Shifts in microphytoplankton species and cell size at Admiralty Bay, Antarctica. *Antarctic Science*, **27**, 1–15, 10.1017/S0954102014000571.

KUIPERS MUNNEKE, P., PICARD, G., VAN DEN BROEKE, M.R., LENAERTS, J.T.M. & VAN MEIJGAARD, E. 2012. Insignificant change in Antarctic snowmelt volume since 1979. *Geophysical Research Letters*, **39**, 6–10, 10.1029/2011GL050207.

LIU, H., WANG, L. & JEZEK, K.C. 2006a. Spatiotemporal variations of snowmelt in Antarctica derived from satellite scanning multichannel microwave radiometer and Special Sensor Microwave Imager data (1978–2004). *Journal of Geophysical Research*, **111**, F01003, 10.1029/2005JF000318.

LIU, H., WANG, L., JEZEK, K.C. & MEMBER, A. 2006b. Automated Delineation of Dry and Melt Snow Zones in Antarctica Using Active and Passive Microwave Observations From Space. **44**, 2152–2163.

LUCKMAN A., ELVIDGE A., JANSEN D., KULESSA B., KUIPERS MUNNEKE P., KING J. & BARRAND N .2014 Surface melt and ponding on Larsen C Ice Shelf and the impact of föhn winds. *Antarctic Science*, **26(6),** 625–635

MARINSEK, S. & ERMOLIN, E. 2015. 10 year mass balance by glaciological and geodetic methods of Glaciar Bahía del Diablo, Vega Island, Antarctic Peninsula. *Annals of Glaciology*, **56**, 141–146, 10.3189/2015AoG70A958.

MAVLYULOV, B.R. 2014. Balans massy l'da lednikovogo kupola Bellingshausen v 2007-2012 (o. King-Dzordz, Udznye Shetlandskie ostrova, Antarctica) [Ice mass balance of Bellingshausen Dome in 2007-2012 (King George Island, South Shetlands Islands, Antarctica)]. *Led I Sneg (Ice and Snow)*, **1**, 27–34.

MOLINE, M.A., CLAUSTRE, H., FRAZER, T.K., SCHOFIELD, O. & VERNET, M. 2004. Alteration of the food web along the Antarctic Peninsula in response to a regional warming trend. *Global Change Biology*, **10**, 1973–1980, 10.1111/j.1365-2486.2004.00825.x.

NAVARRO, F.J., JONSELL, U.Y., CORCUERA, M.I. & MARTÍN-ESPAÑOL, A. 2013. Decelerated mass loss of Hurd and Johnsons Glaciers, Livingston Island, Antarctic Peninsula. *Journal of Glaciology*, **59**, 115–128, 10.3189/2013JoG12J144.

NĘDZAREK, A. 2008. Sources, diversity and circulation of biogenic compounds in Admiralty Bay, King George Island, Antarctica. *Antarctic Science*, **20**, 10.1017/S0954102007000909.

OLIVA, M., NAVARRO, F., HRBÁČEK, F., HERNÁNDEZ, A., NÝVLT, D., PEREIRA, P., RUIZ-FERNÁNDEZ, J. & TRIGO, R. (2017). Recent regional climate cooling on the Antarctic Peninsula and associated impacts on the Cryosphere. Sci. Total Envir., 580, 210-223, doi:10.1016/j.scitotenv.2016.12.030.

OSMANOGLU, B., NAVARRO, F.J., HOCK, R., BRAUN, M. & CORCUERA, M.I. 2014. Surface velocity and mass balance of Livingston Island ice cap ,. *The Cryosphere*, 1807–1823, 10.5194/tc-8-1807-2014.

PFEFFER, W.T., MEIER, M.F. & ILLANGASEKARE, T.H. 1991. Retention of Greenland runoff by refreezing: Implications for projected future sea level change. *Journal of Geophysical Research*, **96**, 22117, 10.1029/91JC02502.

PRITCHARD, H.D., LIGTENBERG, S.R.M., FRICKER, H. A., VAUGHAN, D.G., VAN DEN BROEKE, M.R. & PADMAN, L. 2012. Antarctic ice-sheet loss driven by basal melting of ice shelves. *Nature*, **484**, 502–505, 10.1038/nature10968.

RAU, F. & BRAUN, M. 2002. The regional distribution of the dry-snow zone on the Antarctic Peninsula north of 70° S. *Annals of Glaciology*, **34**, 95–100, 10.3189/172756402781817914.

RYE, C.D., NAVEIRA GARABATO, A.C., HOLLAND, P.R., MEREDITH, M.P., GEORGE NURSER, A. J., HUGHES, C.W., COWARD, A.C. & WEBB, D.J. 2014. Rapid sea-level rise along the Antarctic margins in response to increased glacial discharge. *Nature Geoscience*, **7**, 732–735, 10.1038/ngeo2230.

SCAMBOS, T., HULBE, C. & FAHNESTOCK, M. 2003. CLIMATE-INDUCED ICE SHELF DISINTEGRATION IN THE ANTARCTIC PENINSULA. **76**, 335–347.

SCHLOSS, I.R., ABELE, D., MOREAU, S., DEMERS, S., BERS, A. V., GONZÁLEZ, O. & FERREYRA, G. A. 2012. Response of phytoplankton dynamics to 19-year (1991-2009) climate trends in Potter Cove (Antarctica). *Journal of Marine Systems*, **92**, 53–66, 10.1016/j.jmarsys.2011.10.006.

SKVARCA, P., DE ANGELIS, H. & ERMOLIN, E. 2004. Mass balance of "Glaciar Bahía del Diablo", Vega Island, Antarctic Peninsula. *Annals of Glaciology*, **39**, 209–213, 10.3189/172756404781814672.

STEIG, E.J., SCHNEIDER, D.P., RUTHERFORD, S.D., MANN, M.E., COMISO, J.C. & SHINDELL, D.T. 2009. Warming of the Antarctic ice-sheet surface since the 1957 International Geophysical Year. *Nature*, **457**, 459–462, 10.1038/nature08286.

TEDESCO, M. & MONAGHAN, A.J. 2009. An updated Antarctic melt record through 2009 and its linkages to high-latitude and tropical climate variability. *Geophysical Research Letters*, **36**, 1–5, 10.1029/2009GL039186.

THOMAS, E.R., MARSHALL, G.J. & MCCONNELL, J.R. 2008. A doubling in snow accumulation in the western Antarctic Peninsula since 1850. *Geophysical Research Letters*, **35**, 1–5, 10.1029/2007GL032529.

TORINESI, O., FILY, M. & GENTHON, C. 2003. Variability and trends of the summer melt period of Antartic ice margins since 1980 from microwave sensors. *Journal of Climate*, **16**, 1047–1060, 10.1175/1520-0442(2003)016<1047:VATOTS>2.0.CO;2.

TRENBERTH, K.E., JONES, P.D., AMBENJE, P., BOJARIU, R., EASTERLING, D., KLEIN TANK, A., PARKER, D., et al. 2007. Observations: Surface and Atmospheric Climate Change. *In* Solomon, S., Qin, D., Manning, M., Chen, Z., Marquis, M., Averyt, K.B., Tignor, M. & Miller, H.L., *eds. Climate Change 2007: The Physical Science Basis. Contribution of Working Group I to the Fourth Assessment Report of the Intergovernmental Panel on Climate Change*.

TRUSEL, L.D., FREY, K.E., DAS, S.B., MUNNEKE, P.K. & VAN DEN BROEKE, M.R. 2013. Satellite-based estimates of Antarctic surface meltwater fluxes. *Geophysical Research Letters*, **40**, 6148–6153, 10.1002/2013GL058138.

TURNER, J., COLWELL, S.R., MARSHALL, G.J., LACHLAN-COPE, T. A., CARLETON, A.M., JONES, P.D., LAGUN, V., REID, P. A. & IAGOVKINA, S. 2005. Antarctic climate change during the last 50 years. *International Journal of Climatology*, **25**, 279–294, 10.1002/joc.1130.

VÄLISUO, I., VIHMA, T. & KING, J.C. 2014. Surface energy budget on Larsen and Wilkins ice shelves in the Antarctic Peninsula: results based on reanalyses in 1989–2010. *The Cryosphere*, **8**, 1519–1538, 10.5194/tc-8-1519-2014.

VAN DE BERG, W.J., VAN DEN BROEKE, M.R., REIJMER, C.H. & VAN MEIJGAARD, E. 2005. Characteristics of the Antarctic surface mass balance (1958-2002) using a Regional Atmopsheric Climate Model. *Annals of Glaciology*, **41**, 97–104.

van Wessem, J. M., Ligtenberg, S. R. M., Reijmer, C. H., van de Berg, W. J., van den Broeke, M. R., Barrand, N. E., Thomas, E. R.,Turner, J., Wuite, J., Scambos, T. A., & van Meijgaard, E. 2016. The modelled surface mass balance of the Antarctic Peninsula at 5.5 km horizontal resolution. The Cryosphere. **10**, 271-285.

VAUGHAN, D.G. 2006. Recent Trends in Melting Conditions on the Antarctic Peninsula and Their Implications for Ice-sheet Mass Balance and Sea Level. **38**, 147–152.

VAUGHAN, D.G., MARSHALL, G.J., CONNOLLEY, W.M., PARKINSON, C., MULVANEY, R., HODGSON, D. A., KING, J.C., PUDSEY, C.J. & TURNER, J. 2003. Recent rapid regional climate

warming on the Antarctic Peninsula. *Climatic Change*, **60**, 243–274, 10.1023/A:1026021217991.

WOUTERS, B., HELM, V., FLAMENT, T., WESSEM, J.M. VAN, LIGTENBERG, S.R.M. & BAMBER, J.L. 2015. Dynamic thinning of glaciers on the Southern Antarctic Peninsula. *Science*, **348**, 899–904.

ZWALLY, H.J., ABDALATI, W., HERRING, T., LARSON, K., SABA, J. & STEFFEN, K. 2002. Surface Melt – Induced Acceleration of Greenland Ice-Sheet Flow. 218–223.

Figures

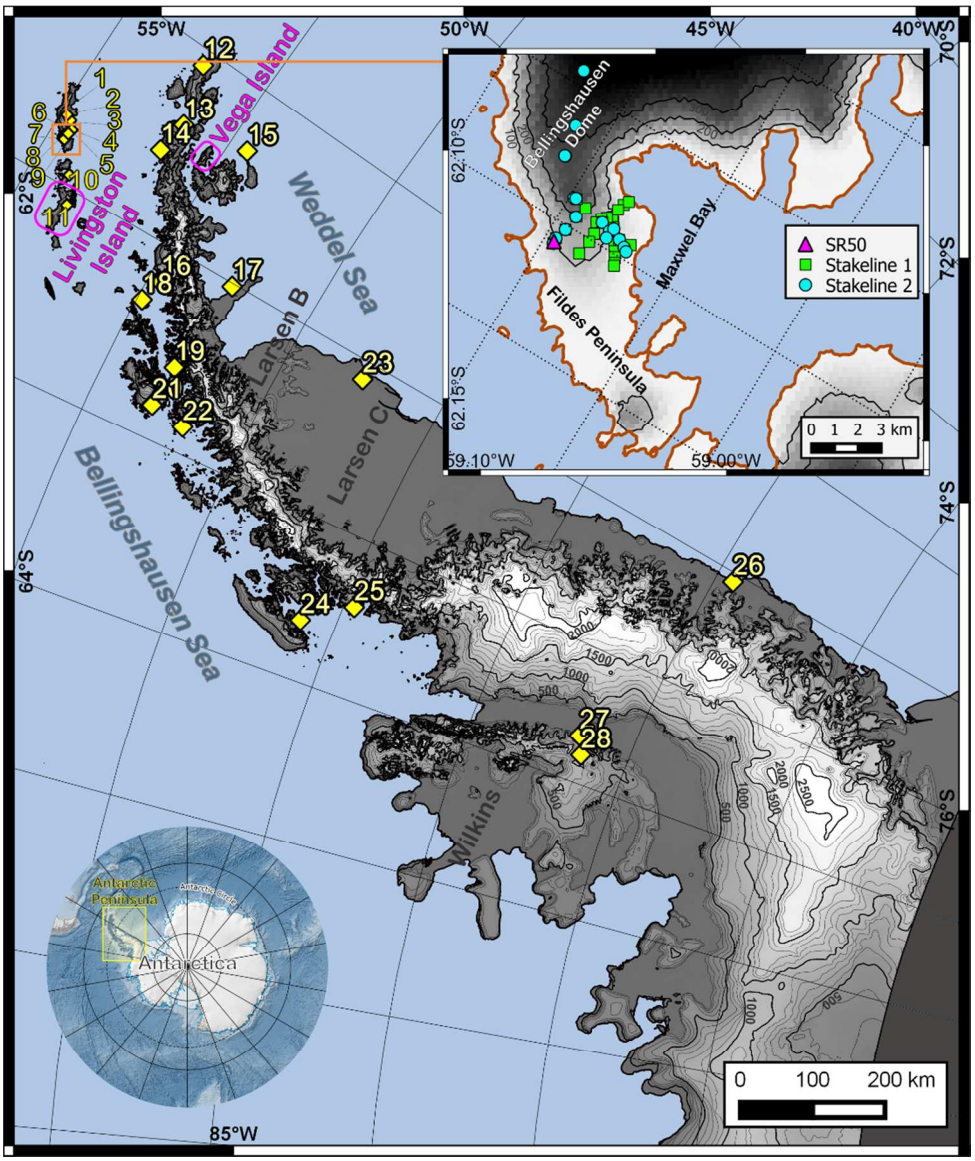

Figure 1: Map showing the study area and data-source distribution. Elevation contours are extracted from RAMP-DEM (Liu *et al*. 2001). Weather stations are represented by yellow diamonds and labelled with numbers, as shown in Table 2. The top right detailed map of King George Island shows the glaciological stakes and ultrasonic ranger used for calibration and validation in the Bellingshausen Dome and the Fildes Peninsula. Magenta squares show locations in Livingston and Vega islands, where long-term surface mass balance records are available.

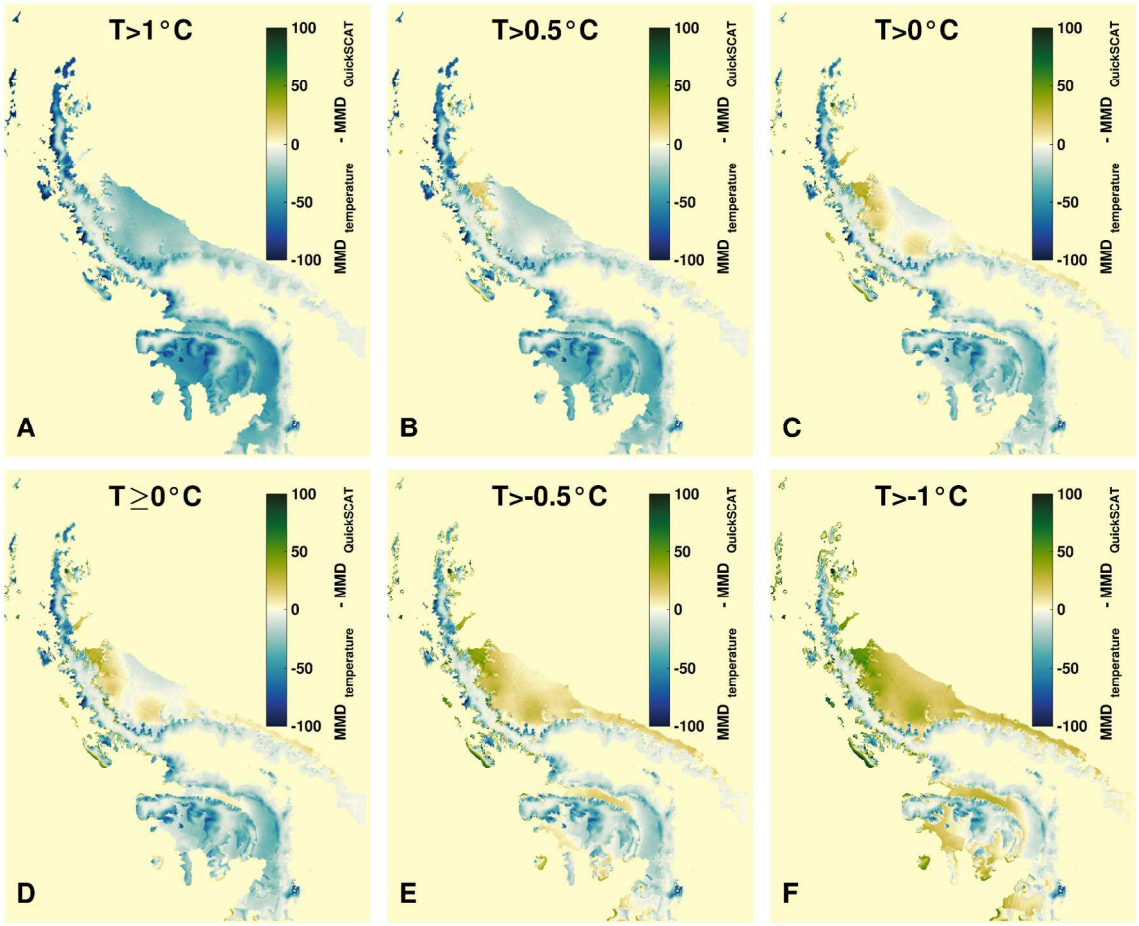

Figure 2: Comparison of the mean melt duration (MMD) derived from **ERAI-based air temperature data against QuickSCAT-derived maps. Six different thresholds are applied to ERAI-derived data to determine the occurrence of melt: A T>1°C, B T>0.5°C, C T>0°C, D T>=0°C, E T>-0.5°C, and F T>-1°C.**

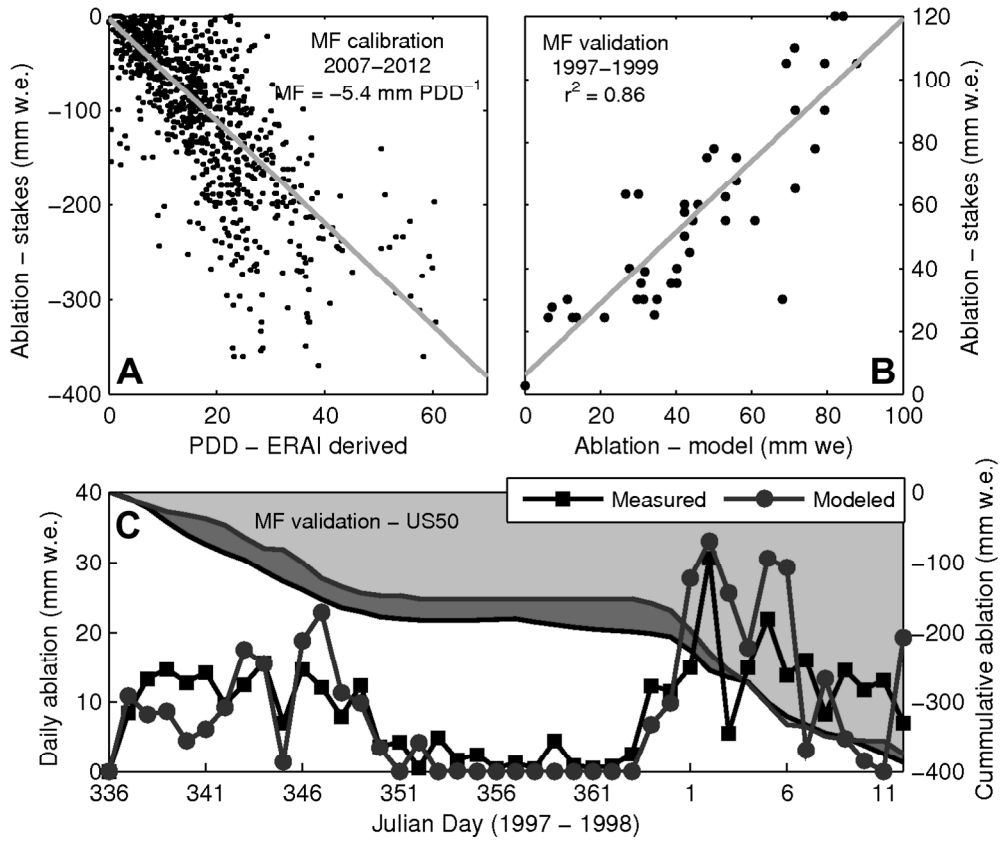

Figure 3: **a** MF estimation, **b** validation against ablation measured at Stake line 2 (1997/1998, 1999/2000) and **c** SR50 (40 consecutive days, from Dec/1997 to Jan/1998)

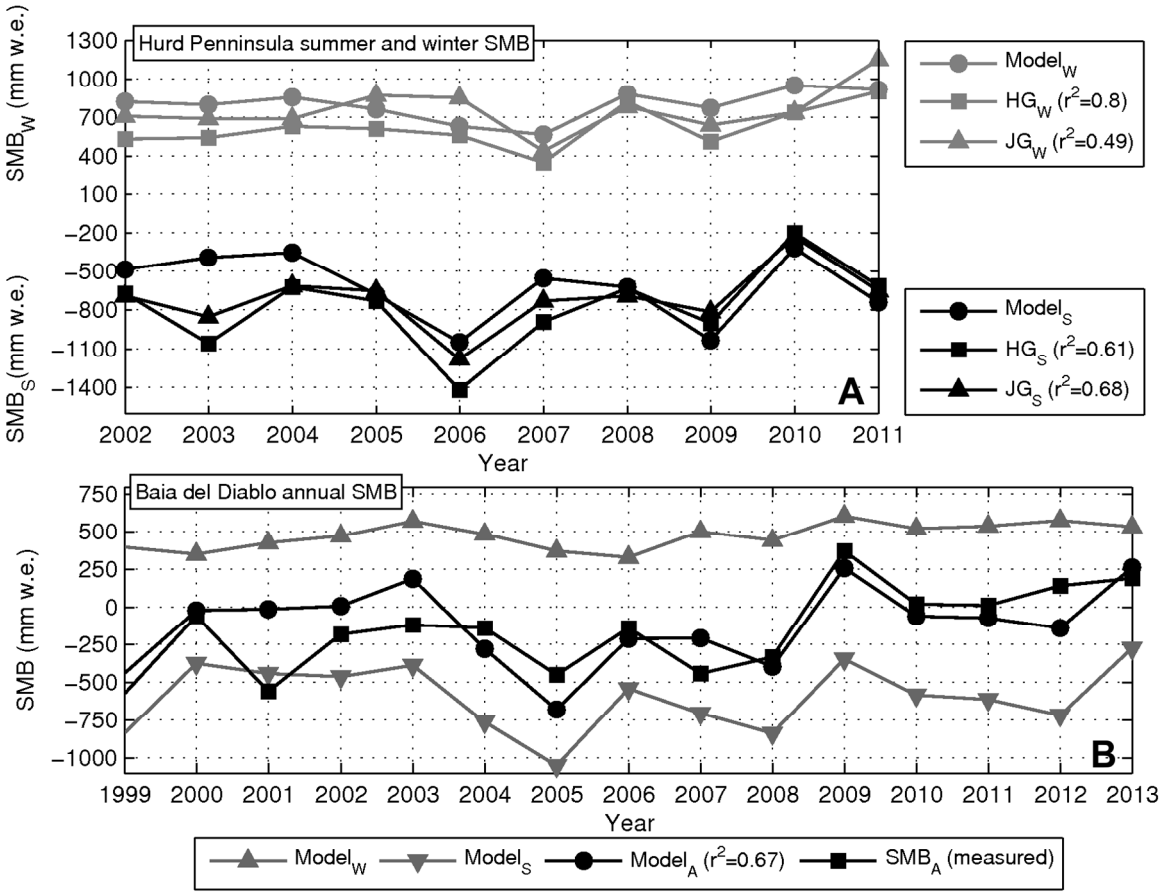

Figure 4: Comparison of modelled area-averaged SMB in: **a** the Hurd Peninsula (Livingston Island) with summer and winter SMB from the Hurd (HG) and Johnsons (JG) Glaciers (Navarro *et al*, 2013) and **b** Baia del Diablo Glacier's (Vega Island) annual SMB (Skvarca et al, 2004; Marinsek and Ermolin, 2015).

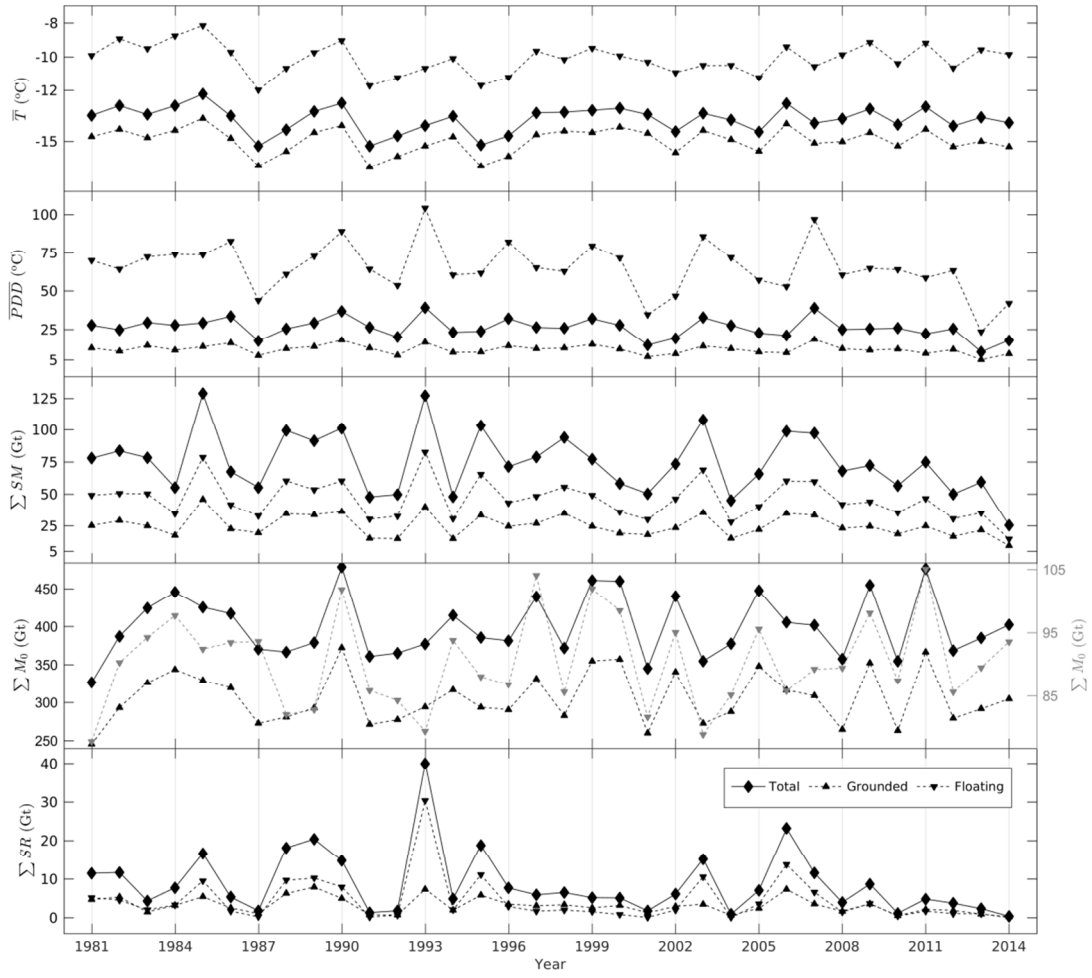

Figure 5: **a** Mean temperature, **b** mean PDDs, **c** total SM, **d** total potential retention and **e** total SR annual time series for the total (continuous line, diamonds), grounded ice (dotted line, upward-pointing triangles) and floating ice (dotted line, downward-pointing triangles) areas. In **d**, the right axis shows scale for the floating area.

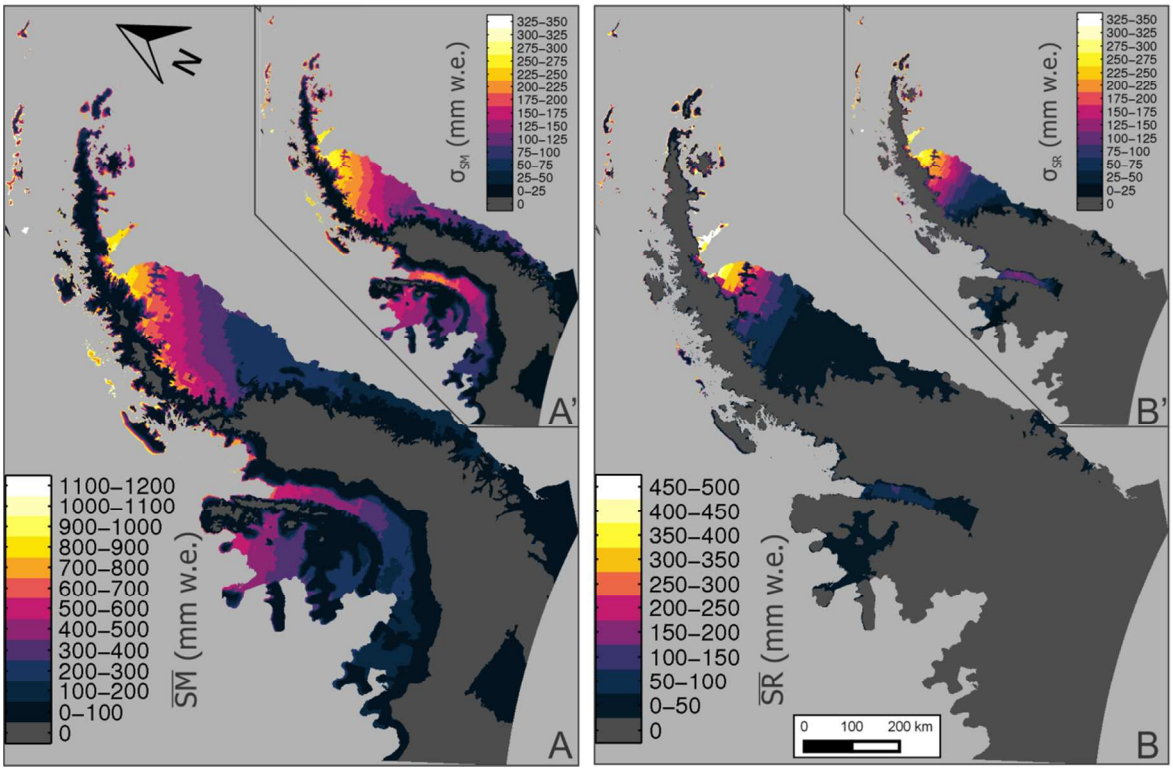

Figure 6: Maps showing: **a** mean SM and its standard deviation (**a'**) over the 1980-2014 period and **b** the mean SR and its standard deviation (**b'**) over the same period.

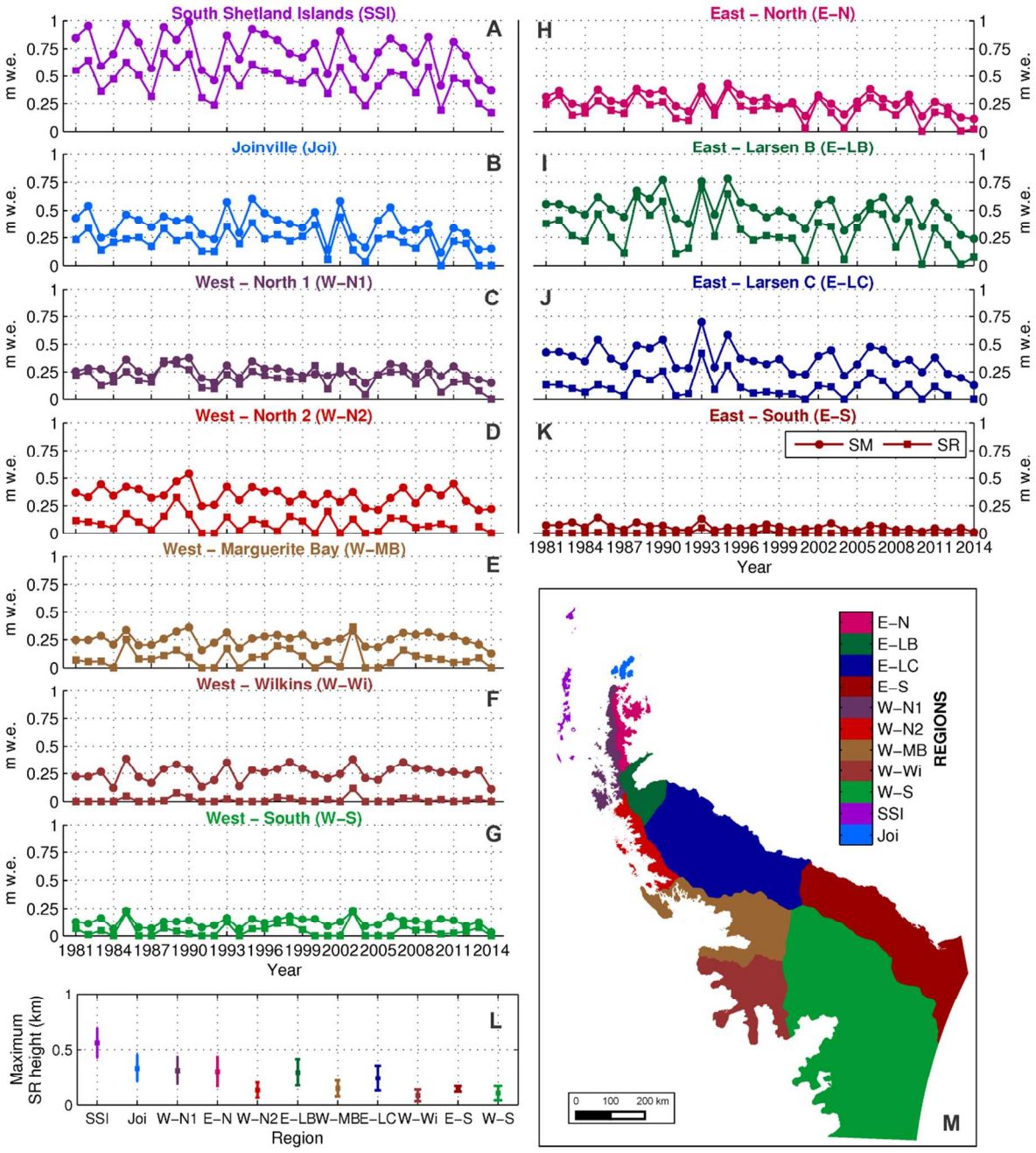

Figure 7: Surface melting (SM) and surface runoff (SR) over the Antarctic Peninsula: **a to k** show the SM (continuous line, circles) and SR (continuous line, squares) time series separated for each AP region; **l** shows the mean and standard deviation of the SR maximum elevation of SR in each region; map **m** delimits each region.

Tables

Table 1: Data used for the calibration and validation of the SM and SR model. KGI denotes King George Island, LIV: Livingston Island, VI: Vega Island, Cal: calibration data, Val: validation data.

Dataset	Type	Period of measurement	Location	Elevation range (m a.s.l.)	Usage	Reference
Weather station	Meteorol. records	Variable (see Tab. 2)	Variable (see Tab. 2)	Variable (see Tab. 2)	Cal	NOAA
Stake line 1	29 ablation stakes	2007-2012	KGI	54-261	Cal	Mavlyulov (2014)
Stake line 2	22 ablation stakes	1997/1998 1999/2000	KGI	85-300 85-205	Val	Braun *et al*. (2001, 2004)
SR50	Ultrasonic ranger	02/12/1997-2/01/1998	KGI	85	Val	Braun *et al*. (2001, 2004)
SMBs	Summer, integrated	2001-2011	LIV	0-370	Val	Navarro *et al*. (2013)
SMBw	Winter, integrated	2001-2011	LIV	0-370	Val	Navarro *et al*. (2013)
SMBa	Annual, integrated	1999-2014	VI	75-630	Val	Skvarca *et al*. (2004), Marinsek & Ermolin (2015)

Table 2: Weather stations used in this study for the validation of PDDs estimated from ERAI. The correlation coefficient and RMSE were calculated between monthly PDDs derived from weather station (WS) measurements and ERAI estimation, excluding the months from April to September.

WS label on map	WS name	Latitude	Longitude	Elevation	Period	Number of months	r^2	RMSE
1	**Ferraz**	-62.08	-58.38	18	2008-2011	18	0.96	146.19
2	**King George**	-62.08	-58.40	267	2001-2002	6	1.00	21.48
3	**Arctowski**	-62.16	-58.46	3	1979-1990	67	0.97	147.08
4	**Jubany**	-62.23	-58.65	20	1980-2014	178	0.98	129.79
5	**King Sejong**	-62.21	-58.75	11	1991-2013	137	0.96	130.42
6	**Dinamet (Uruguay)**	-62.17	-58.83	10	1985-2014	171	0.98	95.62
7	**Bellingshausen**	-62.20	-58.93	16	1979-2014	209	0.98	90.30
8	**Frei (Base)**	-62.25	-58.93	10	1979-1985	39	0.99	88.43
8	**Frei (Station)**	-62.25	-58.93	10	1985-2014	174	0.99	67.95
9	**Great Wall**	-62.21	-58.96	10	1985-2014	173	0.98	87.81
10	**Arturo Prat**	-62.50	-59.68	5	1979-2014	186	0.99	80.11
11	**Juan Carlos**	-62.66	-60.38	10	1989-2014	48	0.90	246.56
12	**Joinville Island**	-63.18	-55.40	75	2007-2013	30	0.97	22.65
13	**Esperanza**	-63.40	-56.98	8	1979-2014	209	0.92	195.08
14	**O'Higgins**	-63.31	-57.90	10	1979-2014	213	0.94	60.52
15	**Marambio**	-64.23	-56.71	198	1979-2014	213	0.93	90.32
16	**Primavera**	-64.17	-60.95	50	1979-1982	19	0.64	110.21
17	**Matienzo**	-64.97	-60.05	32	1979-1987	33	0.96	35.12
18	**Racer Rock**	-64.16	-61.53	17	1991-2006	73	0.92	18.79
19	**Gonzalez**	-64.80	-62.85	10	1981-1982	4	0.98	6.07
20	**Palmer**	-64.76	-64.08	8	1979-2004	97	0.90	225.83
21	**Bonaparte Point**	-64.78	-63.06	8	1997-2014	44	0.97	12.55
22	**Faraday/Vernadsky**	-65.25	-64.26	9	1979-2014	139	0.90	40.52
23	**Larsen Ice Shelf**	-66.96	-60.55	17	1995-2014	115	0.99	6.43

24	**Rothera**	-67.56	-68.13	15	1979-2013	167	0.96	26.96
25	**San Martin**	-68.13	-67.13	4	1979-2014	213	0.84	6.29
26	**Butler Island**	-72.21	-60.33	91	1990-2014	140	0.90	3.16
27	**Fossil Bluff**	-71.33	-68.35	55	1986-2013	74	0.58	0.89
28	**Uranus**	-71.43	-68.93	780	1990-2005	73	0.98	13.44

Point-by-point answers to the reviwers comments

The authors would like to thank both reviewers for their valuable comments and suggestions to improve the quality of the manuscript. We revised the manuscript addressing their comments. All the modifications made in the manuscript are marked in bold. Herein, we present a point-by-point response addressing their comments and respectfully submit to your kind consideration.

Reviewers' Comments to Author:

Reviewer: 1

R: Not sure what the red text in the MS represents: is this a re-submission with highlighted changes compared to a previous version?

A: Yes.

R: English must be significantly improved.

A: The manuscript was submitted to proof read (Elsevier language service) previously to the be submitted to Antarctic Science. Moreover, Dr. Nicholas Barrand is a native English speaker and have also revised the language of the entire text. We would definetely be wiling to improve the language, but it would be very helpfull if the reviewer could kindly provide more specific comments on the expected improvements.

R: Uncertainty estimates for melt and runoff are lacking throughout the MS. Are uncertainties 5%, 10%, 50%?

A: Uncertainties of melt, mass balance and accumulation were added in section **5.2 Downscaling and melt model performance.**

R: Abstract: These numbers are very different from a modelling study that was recently published by Van Wessem and others (2016). That study suggested that a) maximum melt flux of ~50 Gt occurred in 1992, b) maximum runoff occurred in 1992 and did not exceed 20 Gt, c) there is an outspoken negative trend in melt rate. All these three results are at odds with the numbers presented here. Possible reasons should at least be discussed.

A: We discuss the differences compared to Van Wessem and others (2016) and also previous studies in section **6 Discussion**.

In response to the specific (a, b and c) comments of the reviewer, we would like to add the following comments.

In our study, *the years correspond to the melt season that started in November of the previous year* (see line 41, page 12 or MS). Hence, our results of 1993 correspond to November/1992 - October/1993. We adopted this definition to avoid spliting the melt season, because Summer starts in December and lasts until March in the southern hemisphere.

In most years of our study, splitting the melt seasons results in lower peaks of surface melt (see fig. 1) and a considerably different overall behavior of the time series. The data variability suggests that generally there are not two subsequent melt peaks (either positive or negative). For example, our study indicate that the total melt during the calendar year of 1992 was ~118 Gt. Tough, this high value is due to a peak in december/1992, which is part of the 1992/1993 melt season (see fig. 2). On the other hand, the 1991/1992 melt season was not distincly intense.

Our understanding of van Wassen et al (2016) is that their year correspond to the calendar year. That per se will bring up different values in both studies, especially considering the extremely high variability of the melt rates during melt season.

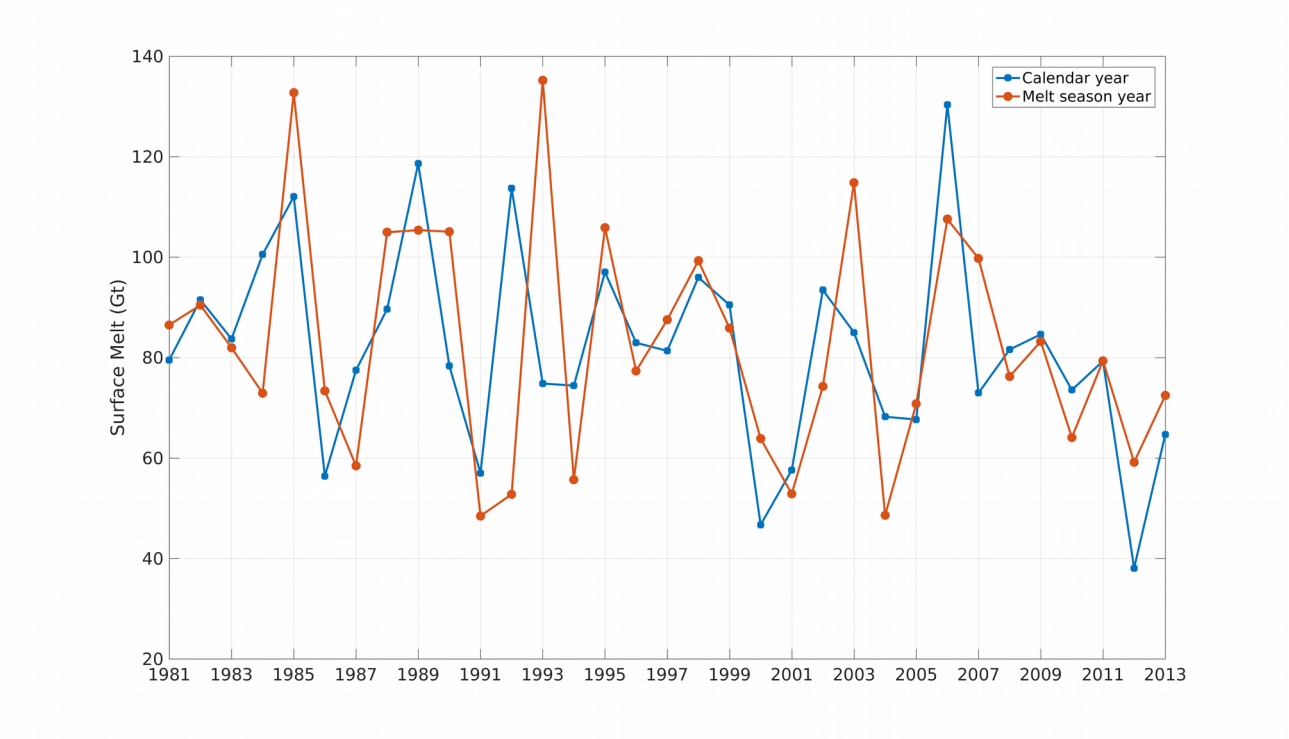

Figure 1 – Comparison of total melt estimates per year considering calendar year (i.e., Jan-Dec, blue), and melt season year (i.e. November/Year-1 – October/Year, red).

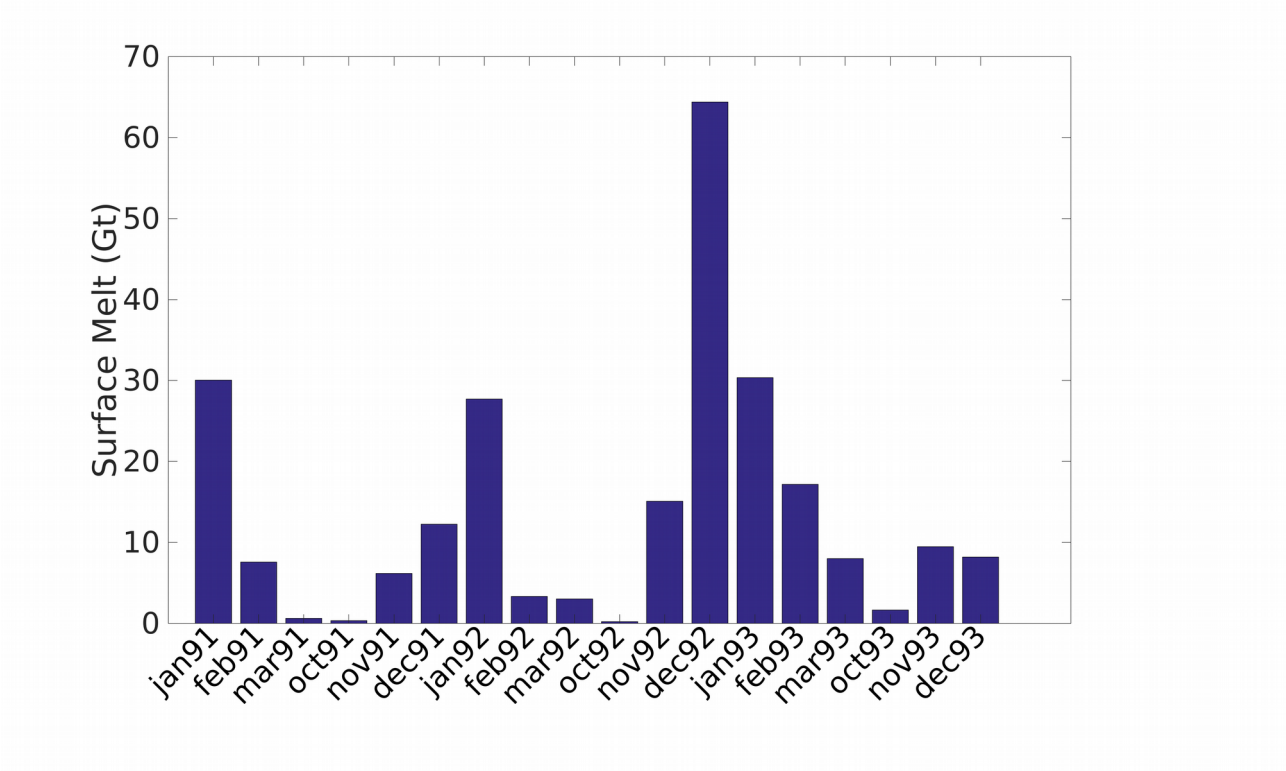

Figure 2 – Total melt estimates by month from jan/1991 to dec/1993.

Furtherly, there must be a misinterpretation of the van Wessem et al (2016) results by the reviewer, because the values presented by van Wessen et al (2016) are different of those indicated by the reviewer comment. Would that be possible that the reviewer looked at the data on figure 7 of their article without noticing that the dashed and continuous line correspond to the eastern and western AP (so the totals would have to be summed for comparing with our results on the entire AP)? The maximum and minimum values are also discussed by the authors (see page 279):

"Of the SMB components (other than RU, that is small), the variability of M is the largest (15 Gt yr−1 , 45 % of the mean), **reaching its peak in 1992 (73 Gt yr−1), and minima (∼ 11 Gt yr−1) in 1986 and 2014**."

"Runoff of meltwater is small but its variability is as high as its mean (4 Gt yr−1); peak years, 1992 and 1995 in particular, reach values of **up to 15 Gt yr−1** , following the peaks in snowmelt."

Another point is that the results of van Wessem et al (2016) regarding meltwater production are quite smaller than previous versions of RACMO estimates and we have not found a direct comparision of the melt estimates provided by RACMO 5.5km against observational or remote sensing derived surface melt.

The validation of RACMO 5.5km is performed against surface mass balance data, and it is clear that precipitation rates dominate the SMB of AP. Hence, it is possible that improvements of SMB estimates

provided by RACMO5.5km (in comparison to RAMCO 27km) may be related to a better representation of precipitation, and not necessarily accompanied by improved representation of snowmelt.

It sounds unlike that an improvement of model resolution and physics would lead to a worst representation of surface melt. However, it is worth noting that:

- The validation results presented in van Wessem et al (2016) are unikely perfomed against highly positive SMB data.

- Comparisons of data from RACMO 27km against QuickSCAT-derived data showed that RACMO 27km underestimates meltflux over Antactica on ~40 Gt (in average) (Trusel et al 2013). The underestimation reached 110 mm we on average in Wilkins ice shelf, for example.

- Melt onset date on Wilkins and Larsen C derived from RACMO 27km data occurs about 40 days later than data derived from QuickSCAT data (Barrand et al, 2013).

- Melt duration is overall underestimated by RACMO 27km compared to QuickSCAT data (Barrand et al, 2013).

- QuickSCAT-derived melt duration is underestimated by ~25 days on Larsen C when compared to Envisat-ASAR-derived data (Luckman et al).

Satellite-derived data suggest that RACMO 27 km derived surface melt is mostly underestimated on the AP. RACMO5.5km provides even lower estimates of surface melt, which are not compared to field measurements neither satellite-derived estimates (to our knowledge).

Regarding the temporal trend, our results (as originally presented) do not have a significant trend. However, if we had considered the calendar year, we would have a significant (99%) decreasing trend of 0.75 Gt $year^{-1}$.

R: p. 6, l. 23: "ERAI is the most recent reanalysis release from ECMWF. It provides data from 1979 to the present in a finest spatial resolution of 0.125 x 0.125." This must be a downscaled product; the native resolution of ERA-Interim is closer to 0.7 degrees. The most recent reanalysis release of ECMWF is ERA5.

A: The authors are thankfull for the comment and changed the information in the manuscript.

R: p. 6, l. 34: The RAMP DEM is an old data product. Why not use more recent DEMs? See for instance: http://dro.dur.ac.uk/20036/

A: We adopted the RAMP DEM product because it provides elevation data on ice shelves.

R: Section 4.1: The main interest of this aper is to reconstruct T2m over the AP. Why then deriving free atmosphere lapse rates and nit T2m lapse rates?

A: This approach was adopted to obtain spatially-variable lapse rates avoiding the effects of the ERA Interim coarse resolution. By calculating the lapse rates between two adjacent ERA interim cells, we would be considering the spatial variation of the temperature entirely as a topographic effect.

R: Section 4.2: if daily temperatures are used, a lower threshold may be preferable, see e.g. doi:10.1029/2010GL044123

A: The threshold used is the one that better performed for deriving melt area (see section).

R: Section 4.2: Using accumulation from ERA-Interim in a topographically complex region as the AP in combination with the highly simplified parameterization of Pfeffer (1991) renders the runoff obtained in this study as unreliable. So it cannot be judged as robust until at least some proof is presented that they are.

A: We removed the "robust" term.

Minor/textual comments

R: p 3, l. 24: I do not see the rationale for introducing the somwhat awkward abbreviation SM. Why not simply M or ME? Similar for runoff.

A: Despite that the authors somwhat agree with the reviewer, the lack of the awkward S in front of M (and R) has been subject of criticism for not stressing that the estimates were exclusively of *surface* melt and runoff produced by *surface* melt. We decided to keep the S to be sure that we are precisely informing what exactly we are presenting, despite its awkwardness.

R: p. 3, l. 41: Not melt, but runoff causes mass loss.

A: The authors are thankfull for the comment and corrected the ms accordingly.

R: p. 4, l. 42: A paper discussing freshwater input into the ocean from the AP is: http://www.sciencedirect.com/science/article/pii/S0967064516303228

A: The authors are thankfull for the reference.

R: p. 6, l. 36: Please avoid use of the phrase "surface air temperature". It is either surface OR air temperature. If you use 2 m temperature, please simply state so. For varying measurement heights, which I assume is the case here, "near surface air temperature" is acceptable.

A: The authors are thankfull for the comment and corrected the ms accordingly.

R: p. 8, l. 52: "Whereas it is recognized that the surface temperature may be a better parameter for estimating the surface melt when compared to the air temperature" This makes no sense. Surface temperature of a melting snow surface is constant, and can therefore not be used to estimate melt variations.

A: The authors are thankfull for the comment and corrected the ms accordingly.

R: p. 11, l. 56: These were stake measurements in ice with known density?

A: Yes.

R: Fig. 5: please use sensible y-axis values in all plots.

A: The authors are thankfull for the comment and corrected the figure accordingly.

Reviewer: 2

The authors would like to greatly thank Dr. Francisco Navarro for the very detailed revision of the MS in terms of both scientific content and language. All modifications suggested by the reviewer are incorporated in the revised version of the MS.